Thermooptically Tuned Cascaded Polymer Waveguide Taps

John M. Taboada[a], Jeffery J. Maki[b], Suning Tang[b], Lin Sun[a], Xuejun Lu[a], and Ray T. Chen[a]

[a] Microelectronics Research Center
The University of Texas at Austin, Austin, TX 78712

[b] Radiant Research, Inc.
3006 Longhorn Blvd Ste 105, Austin, TX 78758-7631

ABSTRACT

Polymer thermooptic waveguide taps have a potential application as light routers for guided wave optical interconnects involving cascaded fanouts. The taps can guide light from an optical bus bar and direct it into other devices in a switching/modulation network. Thermooptic waveguide taps are designed and fabricated on silicon wafers using standard VLSI fabrication techniques. Coupling of light into an adjacent waveguide tap is observed to increase by 12.3% from 38.7% to 51.0% with the application of 34 mW of power.

Keywords: thermooptic tap, polymer waveguide, optical tap

1. INTRODUCTION

Tunable optical waveguide taps are useful for diverting a small fraction of the optical power from a high-power optical source bar to cascaded waveguides serving as the optical power line for optical interconnects. This diverted optical power can provide the wave for a particular optical modulator, while other optical taps derive signal waves from the same source bar for other uses.[1] The thermooptic effect in polymer can provide sufficient index of refraction variation to form a low-voltage tunable optical waveguide tap.[2,3,4] Furthermore, polymer-based optical waveguide taps can be integrated into module-to-module systems using currently available VLSI fabrication techniques.[5,6]

In this paper, we describe our fabrication and performance studies of waveguide taps based on PMMA. With this design, we determine both the coupling efficiency from the source channel to the tap channel and the voltage needed to induce a specific change in the amount of coupling. A schematic of the waveguide-tap structure under investigation is shown in Figure 1.

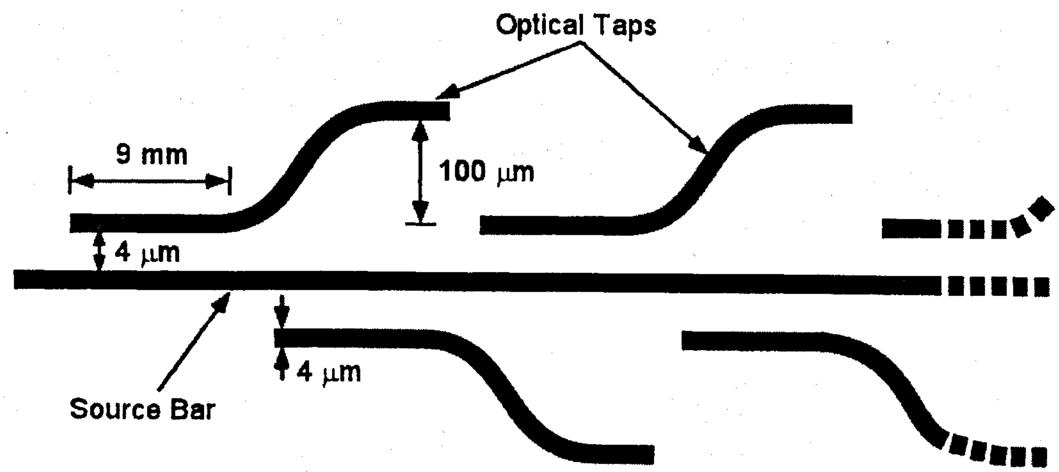

Fig. 1. Schematic of optical waveguide tap structure.

Part of the SPIE Conference on Optoelectronic Interconnects VI
San Jose, California • January 1999
SPIE Vol. 3632 • 0277-786X/99/$10.00

2. BPM SIMULATION

The first step in fabricating a thermooptic tap is to design a channel waveguide that is single mode for the given material system with Norland Optical Adhesive-61 (NOA-61) as the cladding and poly-methyl methacrylate (PMMA) as the waveguiding layer. At 1.3 μm, the index of refraction of the NOA-61 cladding is 1.55 and the index of the PMMA is 1.59. The interaction coupling length, or the length needed to couple light from the source channel waveguide to the tap channel waveguide, is first theoretically determined. We use the beam propagation method (BPM) to determine the channel widths for single mode characteristics at 1.3 μm, and the interaction length and channel separation for coupling. The channel width, depth, and separation are determined to be 4 μm, 1.5 μm, and 4 μm, respectively. The optimized interaction length is also determined to be 9 mm and to have a passive coupling of 35% as is shown in the BPM simulation result in Figure 2. Various waveguide taps were made to these specifications.

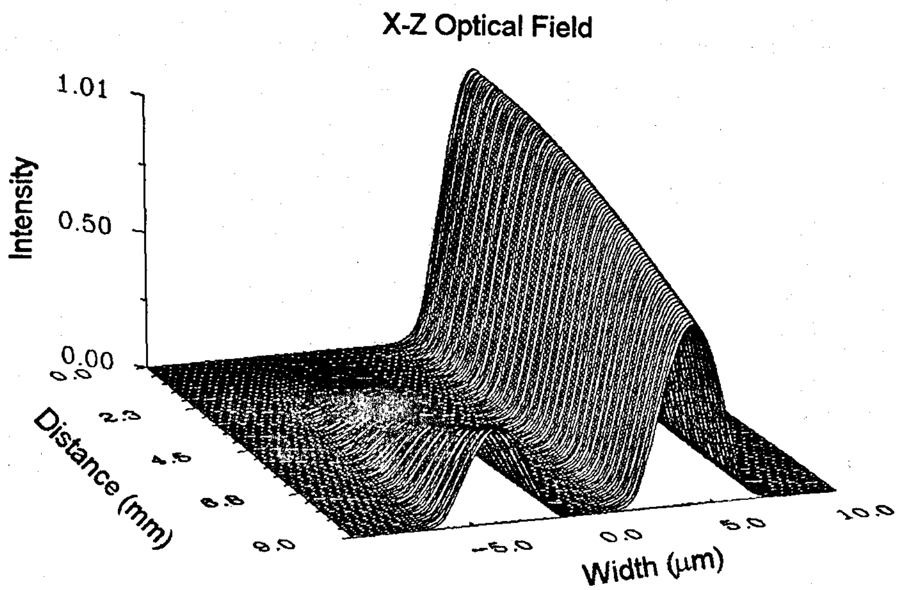

Fig. 2. BPM simulation showing 35% passive coupling after 9mm.

3. DEVICE FABRICATION

The fabrication of thermooptic waveguide taps follows many of the same techniques and equipment used in VLSI fabrication. First, a cladding solution is prepared for spin coating. The solution consists of 1 ml of NOA-61 and 3 ml of cyclopentanone. The solution is stirred for about 5 minutes and then drawn into a syringe. The solution is then UV cured for two minutes and forty five seconds with a UV intensity of about 16 to 20 mW per cm^2 from a UVP Ultraviolet Lamp (Model B100 SP). The solution is then deposited onto a three-inch wafer using a syringe with a 0.2 μm filter. The wafer is then spun using a ramp-up technique. The ramp-up technique consists of several different revolution speeds set for certain amounts of time. First, the wafer is spun at 500 rpm for 30 seconds, then immediately followed, without stopping, by 1000 rpm for 30 seconds. The speed is then increased to 1.5k rpm for 30 seconds and finally to 2k rpm for 60 seconds. The ramp up technique results in a uniform 2 μm cladding layer of NOA-61. The sample is then UV cured for 20 minutes. The core layer consisting of PMMA is then spun coat on top of the bottom-cladding layer using a ramp up technique from 1k to 4k rpm.

Clariant AZ5206 photoresist is then deposited on top of the PMMA and softbaked at 90 °C for 15 minutes. The sample is then patterned with a mask to produce the waveguide taps. The sample with patterned photoresist is developed in AZ425 for about 1 minute and then hardbaked at 125 °C for 1 hour. After hardbaking, the sample is RIE etched with an O_2 plasma. A top NOA-61 cladding layer is spun coat onto the sample using a ramp up technique from 500 to 2k rpm. An AZ5206 photoresist layer is spun coat onto the sample and patterned with a mask of the top electrode structures, which are the conducting pads for the current-induced thermosource. We then develop the photoresist. After deposition of the metal, the sample is dipped into acetone to lift off the metal that was deposited onto the AZ5206 photoresist. Only the metal that was deposited directly onto the top NOA-61 layer remains after this lift-off technique. Finally, the sample is cleaved and polished to facilitate end-fire coupling. The end faces of the sample are polished by using diamond abrasive films with different grit sizes. First, with a 9 μm diamond grit film, the sample is polished for 10 minutes at 90 rpm. Next a film with 6 μm grit is used for 7 minutes at 70 rpm and finally a 3 μm grit film is used for 3 minutes at 40 rpm. This procedure results in a clean, uniform end face. Polishing of the end face was facilitated by using a thick surrounding cladding layer. A schematic and a picture of the cross section are shown in Figures 3(a) and 3(b), respectively. In Figure 3(b), both the top and bottom cladding layers are 10 μm as depicted in the Figure 3(a).

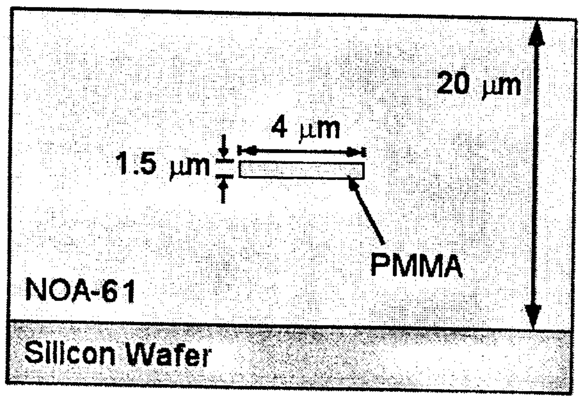

Fig. 3(a). Schematic of cross section.

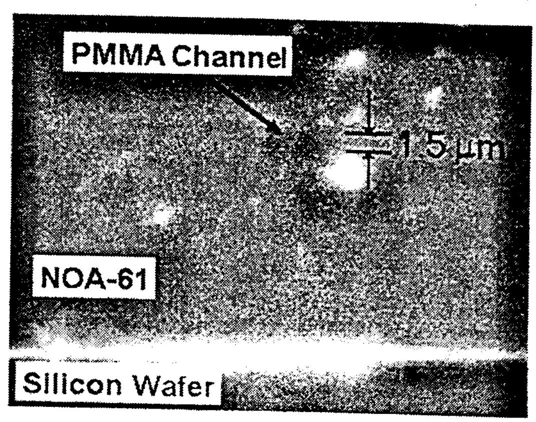

Fig. 3(b). Picture of cross section.

4. EXPERIMENTAL SETUP

We mount the sample on a flexure stage for testing. Light at 1.3 μm is end-fire coupled into the main source bar waveguide defined in Figure 1. The light coupled through the guides is then imaged onto a screen. An IR camera is focused onto the screen and an image of the waveguide core is displayed on a video monitor to observe the light passing through the channel waveguides. We effectively view the near field light emerging from the waveguide. Contacts to the metal pads on the sample are made with two *xyz* needle-point positioners mounted to the sides of the sample stage. A 30 V power supply is connected across the two contact pads of the electrode. A 1 kΩ resistor is also connected in series with the top metal electrode. A voltmeter is used to measure the voltage drop across the resistor in order to determine the current flowing through the top metal electrode. A photograph of the end-fire-coupling setup and a schematic of the setup are shown in Figures 4(a) and 4(b), respectively.

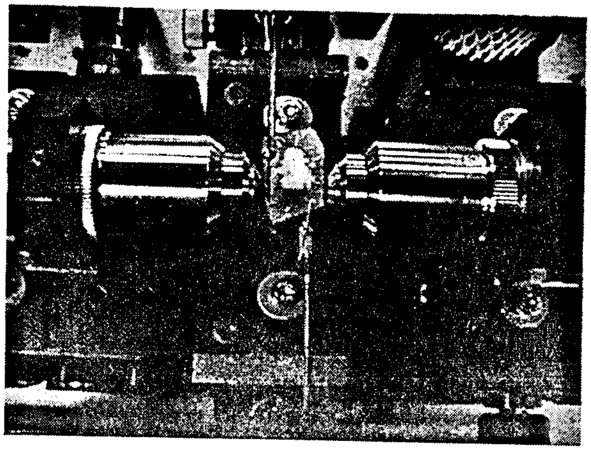

Fig. 4(a). Butt-coupling setup.

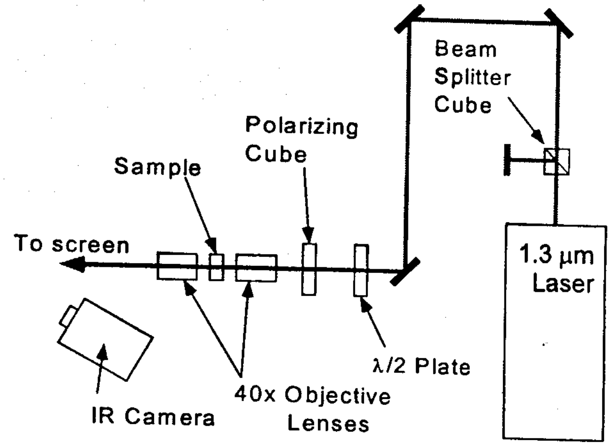

Fig. 4(b). Schematic of the setup.

5. EXPERIMENTAL RESULTS

Light at 1.3 μm is first coupled into the source bar waveguide. The adjacent channels of the waveguide taps are separated by 4 μm. Some light is coupled into the adjacent channel without applying a voltage to heat the device. The IR camera is focused on the screen and the video signal is fed into a display monitor and a Spiricon Beam Analyzer. Contacts are made to the electrode pads that are on top of the source bar channel waveguides in series with a 1 kΩ resistor. The power supply is set at 15 volts and the voltage measured across the 1 kΩ series resistor is 11.5 volts or 11.5 mA is flowing through the drive electrode. The resistance of the chromium-gold drive electrode is measured to be 260 Ω. Thus, 3 volts are applied across the two contact pads of the drive electrode and the electrical power consumption for the optical tap is about 34 mW. The output data is recorded and analyzed for two waveguide taps, with and without heat. Figures 5(a) and 5(b) show the spots imaged on the screen for the waveguide taps with heat and no heat. The brighter peak in Figure 5(a) is the source

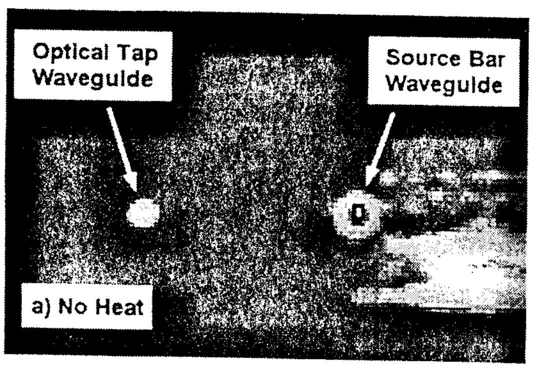

Fig. 5(a). Near field imaged output with no heat showing 38.7% coupling.

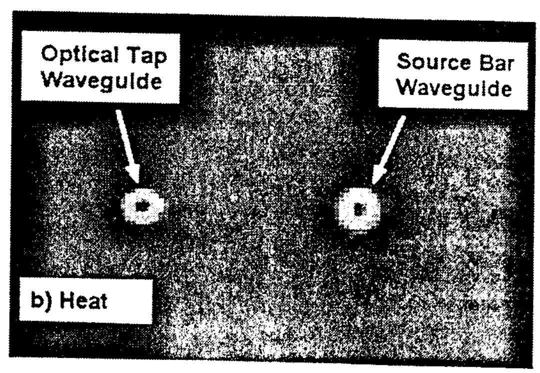

Fig. 5(b). Near field imaged output with heat showing 51.0% coupling.

channel bar of the thermooptic taps. Intensity profile data is extracted from the captured images and graphed in Figure 6. The area under the curve is calculated and then used to determine the percent coupling with and without the application of heat. The optical tap in Fig. 5(a) is determined to have passive coupling of 38.7%. When 34 mW of electrical power is applied to this tap, the coupling increases to 51.0%. A tap waveguide device under the same fabrication conditions shows a consistent tap ratio along the cascaded tap guides. The coupling efficiency (source bar to tap) is designed to be low compared to a conventional directional coupler. This is so because of the need of cascaded fanout for several tap channels. The tunable range from 38.7% to 51.0% provides us with a better control of distributing the optical power with an even fanout. A larger dynamic range can be realized also by employing different power levels and channel separations.

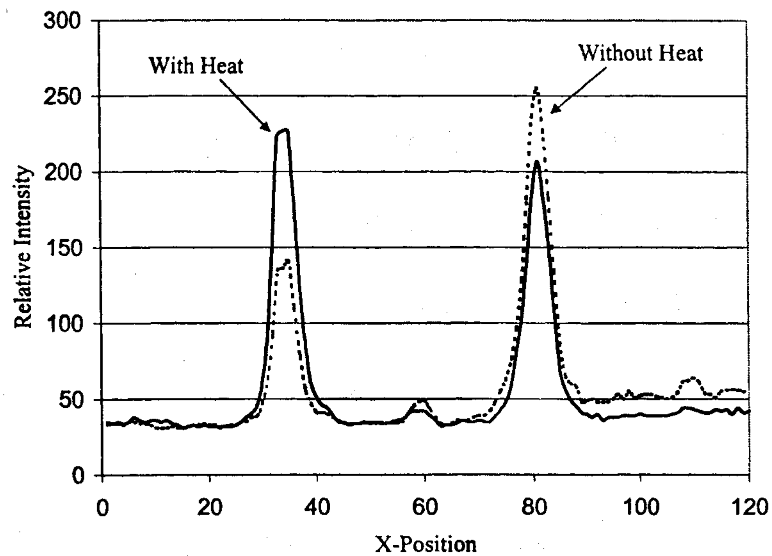

Fig. 6. Intensity profile of Figures 4(a) and (b) showing 38.7% and 51.0% coupling, respectively, for the case with no heat and heat.

6. CONCLUSIONS AND FUTURE WORK

In summary, polymer thermooptic taps are designed and fabricated to operate at 1.3 μm. Using a beam analyzer, the coupling between channels of cascaded waveguide taps are observed to change with the application of 34 mW of power to a top electrode heater. By applying power to the electrode, coupling could either be increased or decreased, depending on the position of the heater element. In one of the cases, the coupling increased 12.3% from 38.7% to 51.0% with the application of 34 mW of power to the top electrode. Future improvements could be to use an adjacent channel, opposite the optical tap. By using this design, the other optical taps down the rail will see a constant light signal in the rail with a minimum fluctuation among taps up the optical rail.

ACKNOWLEDGEMENTS

This research is sponsored by the AFOSR, the BMDO, the DARPA's Center for Optoelectronics Science and Technology (COST), the 3M Foundation, and the ATP program of the State of Texas.

REFERENCES

1. T. E. Van Eck, A. J. Ticknor, R. S. Lytel, and G. F. Lipscomb, "Complementary optical tap fabricated in an electro-optic polymer waveguide," *Applied Physics Letters*, 58, 1588 (1991).
2. Y. Hida, H. Onose, and S. Imamura, "Polymer Waveguide Thermooptic Switch with Low Electric Power Consumption at 1.3 μm," *IEEE Photonics Technology Letters*, vol. 5, no. 7, pp. 782-784, July 1993.
3. M. B. J. Diemeer, J. J. Brons, and E. S. Trommel, "Polymer Optical Waveguide Switch Using the Thermooptic Effect," *Journal Lightwave Technology*, vol.7, no. 3, pp. 449-453, March 1989
4. K. Hashimoto, Y. Nakamura, M. Yamaguchi, and H. Kogo, "High-Performance Optical Switch Using Thermo-Optic Effect," *Electronics and Communications in Japan*, part 2, vol. 69, no. 4, 1986.
5. T. Jannson, R. T. Chen, and F. Lin, "Optoelectronic Chips and Multi-chip Modules," *IEEE and Electronic Industries Association, 42nd Electronic Components and Technology Conference*, 92-P003.
6. N. Keil, H. H. Yao, C. Zawadzki, and B. Strebel, "4x4 polymer thermo-optic directional coupler switch at 1.55 μm," *Electronics Letters*, vol. 30, no. 8, pp. 639-640, April 1994.

Further author information -
J.M.T.: Email: taboada@ccwf.cc.utexas.edu; Telephone: 512-232-2586; Fax: 512-471-8575
J.J.M.: Email: maki@radiant.com
S.T.: Email: suning@mail.utexas.edu
L.S.: Email: lsun@ece.utexas.edu
X.L.: Email: xjlu@ece.utexas.edu
R.T.C.: Email: raychen@uts.cc.utexas.edu